Chinese Chemical Letters 34 (2023) 108209

Contents lists available at ScienceDirect

Chinese Chemical Letters

journal homepage: www.elsevier.com/locate/cclet

Autocatalytic strategy for tuning drug release from peptide-drug supramolecular hydrogel

Yuqin Wu, Tian Xia, Xiaohui Ma, Lei Lei, Lulu Du, Xiaoning Xu, Xiangyi Liu, Yueting Shi, Xingyi Li*, Deqing Lin*

Institute of Biomedical Engineering, School of Ophthalmology & Optometry and Eye Hospital, Wenzhou Medical University, Wenzhou 325027, China

ARTICLE INFO

Article history:
Received 14 November 2022
Revised 3 February 2023
Accepted 8 February 2023
Available online 11 February 2023

Keywords:
Peptide-drug conjugates
Supramolecular hydrogel
Autocatalysis
Hydrolysis
Drug release

ABSTRACT

Peptide-drug conjugates (PDCs) composed of peptide, spacer and drug have gained extensive attention in the field of drug delivery owing to its precise control over the drug payload and architecture. However, the achievement of controllable and rapid drug release at targeted site by PDCs is still a great challenge for pharmaceutist. Herein, we introduced the histidine residue into PDCs to generate a supramolecular hydrogel *via* a pH-trigger strategy, which exhibited an autocatalytic effect to precisely tune drug release from PDCs hydrogel. Using indomethacin (Idm) as model drug, various PDCs (Y(Idm)EEH, Y(Idm)EEK and Y(Idm)EER) were synthesized and their self-assembling properties were investigated in terms of critical aggregation concentration (CAC), transmission electron microscopy (TEM) and rheometer. Introduction of histidine residue into PDCs presented a robust catalytic activity on the ester hydrolysis of *p*-nitrophenyl acetate in aqueous solution, as well conferred the autocatalytic capacity to hydrolyze the PDCs into active parent drug (Idm). Overall, we reported an autocatalytic activity of histidine residue to precisely tune drug release from PDCs hydrogels.

Peptide-drug conjugates (PDCs) acting as an emerging class of prodrugs formed by the covalent conjugation of a peptide sequence to a drug *via* a cleavable linker, have gained considerable attention in the field of drug delivery [1–7]. Owing to the excellent biocompatibility, biodegradability, and multifunctionality of peptide units, the PDCs with favorable properties of the overall conjugate amphiphilicity and ionization could be rationally designed and synthesized [8–13]. With the assistance of peptide units, the solubility as well as stability of the drug were greatly improved in the terms of amphiphilic PDCs. Moreover, PDCs supramolecular hydrogels could be generated *via* the spontaneous or stimuli instructed assembly strategies to realize the efficient local and targeting drug delivery [14–18]. To further achieve precise targeting drug delivery at desired lesion, a biodegradable linker (*i.e.,* ester bond, hydrazone bond, amide bond) in response of the unique microenvironment was generally integrated into PDCs, which is conducive to on-demand release of parent drug at targeted site [19–21]. Among these biodegradable linkers, ester linkages have been extensively implemented in various PDCs owing to the different types of esterase distributing in the living system [22]. The rate of biotransformation from PDCs is extremely important because it acts as central role for the intensity of drug action [23,24]. However, due to the stereo-hindrance effect of different PDCs and substrate selectivity of esterase, the bioconversion rates of PDCs varied significantly.

Pilot studies have been documented that the utilization of imidazolyl groups in artificial catalysts have been popular given the histidine played a vital role in the catalytic activity of the enzymes including esterase, lipase, trypsin and elastase [25–28]. More recently, histidine based amphiphilic nanomaterials (*i.e.*, nanofiber, nanotube, nanosphere) to mimic the natural enzymes have been reported to catalyze the ester hydrolysis [29–34]. Inspiring by these studies, we intended to integrate the histidine into PDCs as potential autocatalysts for ester hydrolysis to tune drug release from supramolecular hydrogel. We firstly synthesized a drug-peptide amphiphile (Y(Idm)EEH) containing a histidine at the terminal position to confer catalytic activity, and mutated histidine by lysine or arginine to generate inactive analogs (Y(Idm)EEK and Y(Idm)EER) [35–37]. We thereafter investigated the self-assembly behavior of these PDCs and measured their critical aggregation concentrations (CAC). Moreover, we presented the catalytic activity of these amphiphiles using the model ester *p*-nitrophenyl acetate as the substrate and measured their autocatalytic activity in an aqueous solution.

* Corresponding authors.
E-mail addresses: lixingyi_1984@mail.eye.ac.cn (X. Li), dq.lin@wmu.edu.cn (D. Lin).

https://doi.org/10.1016/j.cclet.2023.108209
1001-8417/

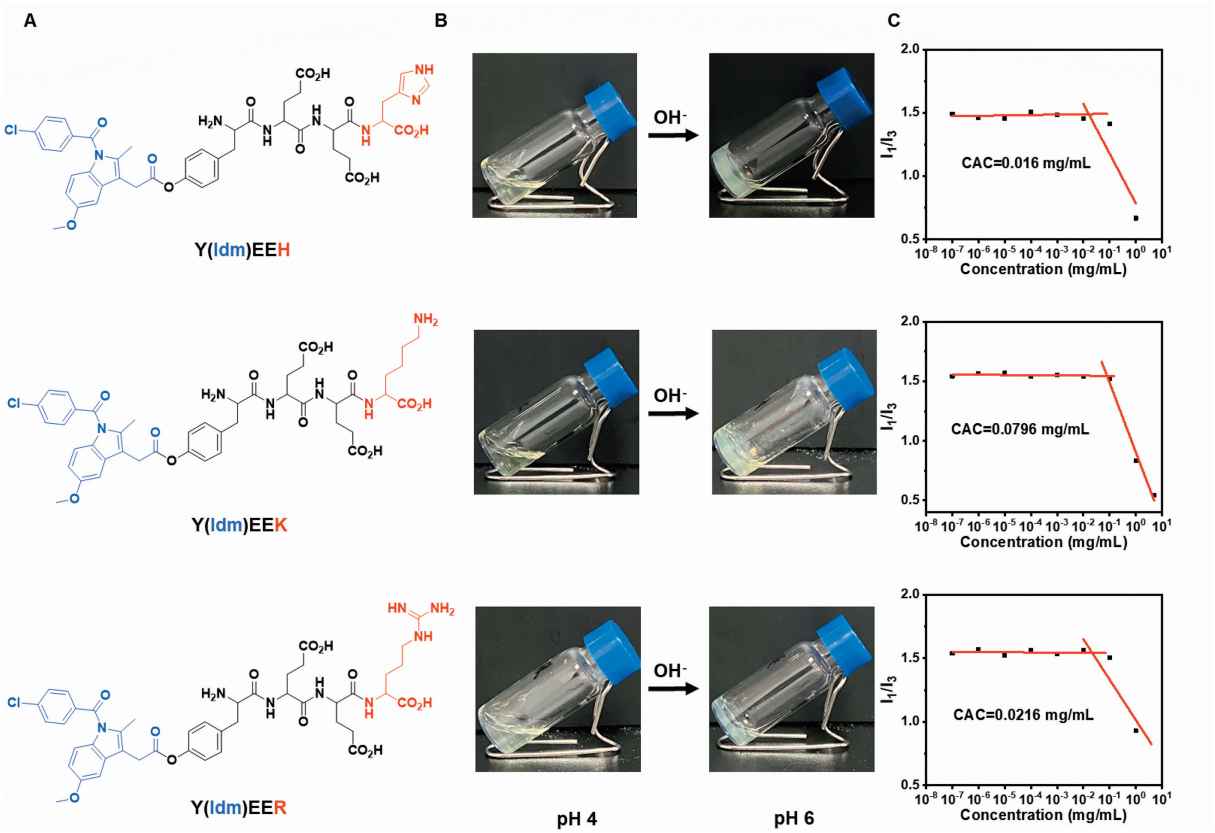

Fig. 1. (A) Chemical structure of Y(Idm)EEH, Y(Idm)EEK and Y(Idm)EER. (B) pH-induced hydrogelation of various PDCs. (C) Critical aggregation concentration (CAC) values of various PDCs.

Different PDCs (Fig. 1A) were synthesized using a classical SPPS method and their identities were further identified by LC-MS and ^{1}H NMR (Figs. S1–S6 in Supporting information). These compounds with identity over 95% were purified by reversed phase HPLC. The histidine residue in PDCs was mutated by lysine or arginine residues to assess their self-assembly behavior and catalytic ability. All these PDCs were found to be soluble in water to generate clear solutions at pH 4, and formed semi-transparent supramolecular hydrogels at their concentrations over 2.5 mg/mL (MGC) as adjusting pH value to 6–7 (Fig. 1B). When pH value was raised to >7, the formed hydrogels dissolved and turned into a clear solution again. Gel formation strongly indicated the robust self-assembly capacity of these PDCs and the mutation of histidine residue by lysine or arginine residue did not affect their self-assembly behavior of PDCs. The CAC values of Y(Idm)EEH, Y(Idm)EEK and Y(Idm)EER hydrogel were 0.016, 0.0796 and 0.0216 mg/mL (Fig. 1C).

TEM was adopted to visualize micro-morphology of PDCs assemblies at different pH conditions and different concentrations. As shown in Figs. 2A–C, it was clearly observed that Y(Idm)EEH, Y(Idm)EEK and Y(Idm)EER aqueous solutions (10 mg/mL) had a loose nanofibril structure at pH 4. With pH condition increasing to 6–7, the Y(Idm)EEH, Y(Idm)EEK and Y(Idm)EER hydrogels (10 mg/mL) formed spontaneously, which were primarily composed of high-aspect-ratio nanofibers entangling with each other to form a network accompanied with the existence of some nanospheres (Figs. 2D–F). The denser nanofibril structure formed in PDCs hydrogel at pH 6, which might be related to disappearance of the electrostatic barrier between nanofibers upon an increase of pH value. Interestingly, the Y(Idm)EEH, Y(Idm)EEK and Y(Idm)EER aqueous solutions (200 μmol/L) at pH 6 exhibited a uniform nanosphere morphology rather than nanofibril structure (Fig. S7 in Supporting information). It seems to suggest that there is a micro-

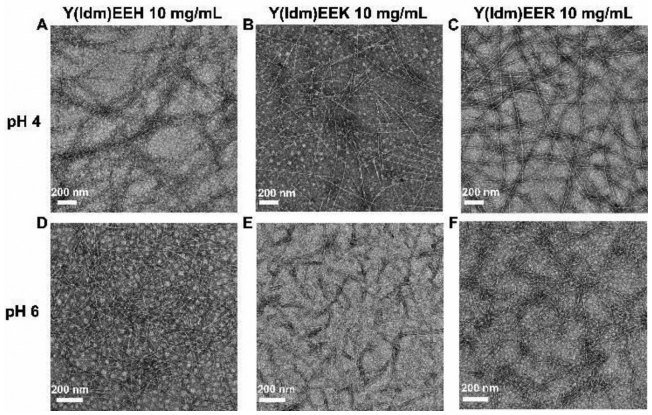

Fig. 2. TEM images of (A) Y(Idm)EEH, (B) Y(Idm)EEK and (C) Y(Idm)EER aqueous solutions (10 mg/mL) at pH 4. TEM images of (D) Y(Idm)EEH, (E) Y(Idm)EEK and (F) Y(Idm)EER hydrogels (10 mg/mL) at pH 6. Scale bar: 200 nm.

morphological transition from nanosphere to nanofibers with an increase of PDCs concentration.

We thereafter used the rheometer to investigate the rheological properties of various PDCs hydrogels (Y(Idm)EEH, Y(Idm)EEK and Y(Idm)EER). As presented in Fig. 3, all the tested hydrogels exhibited the bigger storage modulus (G') values over their corresponding loss modulus (G'') values at the frequency range from 0.1 rad/s to 100 rad/s, suggesting the viscos-elasticity of hydrogels. Strain sweep (Fig. 3) indicated that the mechanical properties of all hydrogel samples decreased significantly with an increasement of strain. The failure strain of hydrogel can be regarded as the crossover of G' and G'' value and the hydrogel turns

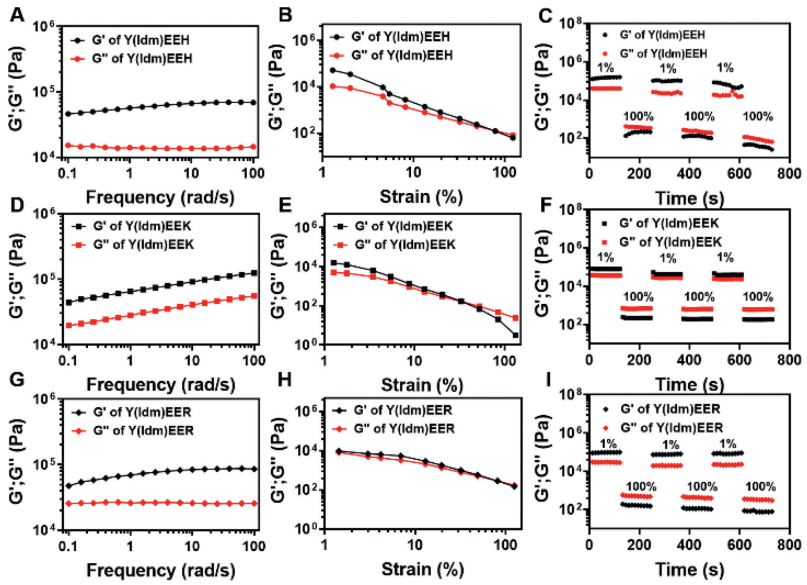

Fig. 3. Rheological properties of (A–C) Y(Idm)EEH, (D–F) Y(Idm)EEK and (G–I) Y(Idm)EER hydrogels (10 mg/mL) at pH 6.

into a viscous liquid. Notably, the failure strain of Y(Idm)EEH and Y(Idm)EER hydrogels was about 50% strain, which is much higher than that of Y(Idm)EEK hydrogel (approximately 30% strain). This result might be explained by that the nanofibers of Y(Idm)EEH and Y(Idm)EER hydrogels were relatively longer and denser than those of Y(Idm)EEK hydrogel.

One of the great advantages of supramolecular hydrogel is the capacity of mechanical property to recover quickly after failure. To test this, we performed two individual strains sweep from 1% to 100% with 800 s recovery periods between the strains. As shown in Fig. 3, all the tested hydrogel samples turned into liquid state as strain approaching to 100%, and recovered rapidly to hydrogel state after the transition to 1% strain. The self-healing property of these PDCs hydrogels indicated that the non-covalent interactions (*i.e.,* hydrogen bond) were able to quickly reform after breaking during large strains (100%). Overall, the self-healing property and the resistance to cyclic strain render these hydrogels great applicable in biomedical field which require recovery after significant deformation, such as injectable therapies.

The catalytic activity of various PDCs was measured by detecting the production of hydrolytic product 4-nitrophenol using 4-nitrophenal acetate as substrate (Fig. 4A). In the PBS solution (Figs. 4B and C), the hydrolytic reaction was very slow and the kinetics profile was linear. This might be attributed to the fact that the hydrolysis underwent a general acid-base catalysis primarily mediated by the weakly alkaline condition of PBS (pH 7.4). Similarly, Y(Idm)EEK and Y(Idm)EER as catalysts led to results close to the PBS alone (Figs. 4B and C), indicating that both Y(Idm)EEK and Y(Idm)EER do not present any obvious catalytic activity. Interestingly, the presence of Y(Idm)EEH resulted in a significant increasement of the hydrolytic rate, which was close to the catalytic activity of cell lysate (2×10^6 cell/mL) from Raw264.7 macrophage. Moreover, we also measured the hydrolytic rate catalyzed by different Y(Idm)EEH concentrations, and found that the hydrolytic rate increased with an increase of Y(Idm)EEH concentration (Fig. S8 in Supporting information). Notably, the hydrolytic rates catalyzed by 200 and 400 μmol/L Y(Idm)EEH were significantly higher than that of cell lysate from Raw264.7 macrophage, implying the robust catalytic activity of Y(Idm)EEH. Based on these results, it is reasonable to believe that the catalytic activity of Y(Idm)EEH was attributed to the existence of abundant reactive H residues on the surface of the nanostructures. We thereafter measured the hydrolytic kinetics of various PDCs. Plots of the initial rate versus substrate concentration were presented (Fig. 4D). According to the Michaelis-Menten equation, the apparent kinetic parameters were calculated (Fig. 4E) and the results showed that the catalytic efficiencies (k_{cat}/K_m) for Y(Idm)EEH is 0.087 $(mol/L)^{-1}$ s^{-1}, which is close to the k_{cat}/K_m value of cell lysate from Raw264.7 macrophage (0.12 $(mol/L)^{-1}$ s^{-1}). This value exceeds by 6-folds as compared to those of Y(Idm)EEK, Y(Idm)EER and PBS. Overall, the proposed Y(Idm)EEH exhibited an enhanced catalytic rate and efficiency over than that of Y(Idm)EEK and Y(Idm)EER.

Since the Idm was covalently conjugated with peptide *via* an ester linkage, we thereafter evaluated the autocatalytic efficacy of PDCs to generate its parent drug. As shown in Fig. 5A and Fig. S9 (Supporting information), all the tested hydrogel samples (Y(Idm)EEH, Y(Idm)EEK and Y(Idm)EER) did not undergo apparent hydrolysis to release native Idm as storage at 4, 25 and 37 °C for 7 days. This might be ascribed to the fact that the ester bond buried into nanofibers, which could not be hydrolyzed by weakly alkaline PBS or H residue in PDCs. However, diluted Y(Idm)EEK and Y(Idm)EER solutions underwent an apparent hydrolysis to release native Idm as incubating in PBS (pH 7.4) for 48 h (Fig. 5B). An enhanced hydrolysis of Idm from PDCs by PBS should be attributed to higher exposure of reactive sites in diluted solutions. More importantly, Y(Idm)EEH exhibited a more profound hydrolytic effect to yield a relative higher Idm conversion, which might be related to the robust catalytic capacity of H residue in Y(Idm)EEH. Thus, the introduction of histidine residue into PDCs could tune drug release *via* the autocatalytic strategy.

In conclusion, a series of amphiphilic PDCs (Y(Idm)EEH, Y(Idm)EEK and Y(Idm)EER) were synthesized and self-assembled into supramolecular hydrogel spontaneously as tuning pH condition to 6–7. All the formed PDCs hydrogels were composed of nanofibers and exhibited resembled rheological properties. The PDCs containing histidine residue brought a potent catalytic activity on the ester hydrolysis of *p*-nitrophenyl acetate in aqueous solution and the hydrolytic efficiency was comparable with that of cell lysate from Raw264.7 macrophage. Moreover, the introduction of histidine residue in PDCs conferred the robust autocatalytic capacity to hydrolyze the PDCs into active parent drug form, thus offering a strategy to tune drug release from PDCs hydrogel.

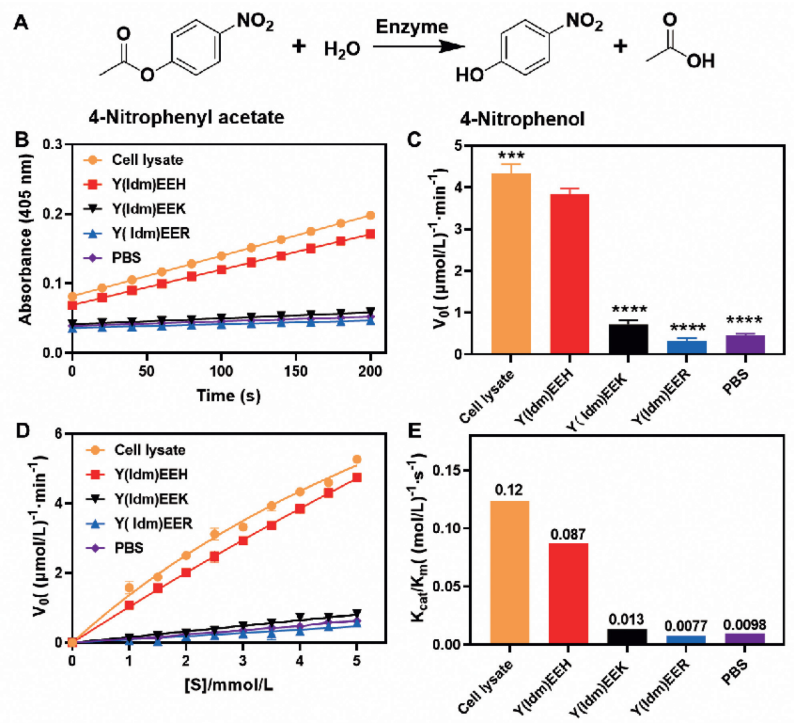

Fig. 4. (A) Hydrolysis reaction of 4-nitophenyl acetate (4-NPA) in aqueous solution. (B, C) Evalution of 4-nitophenyl acetate (4-NPA) conversion into 4-nitophenyl (4-NP) in the presence of various PDCs (200 μmol/L). Cell lysate: 1 mL cell lysate from 2×10^6 Raw 264.7 macrophages; $^{***}P = 0.0003$,$^{****}P < 0.0001$ *vs.* Y(Idm)EEH. (D, E) Measurement of k_{cat}/K_m ($(mol/L)^{-1}$ s^{-1}) according to the Michaelis-Menten equation.

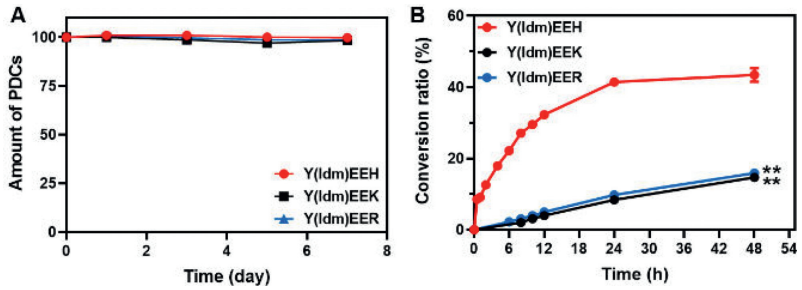

Fig. 5. (A) The chemical stability of Y(Idm)EEH, Y(Idm)EEK and Y(Idm)EER hydrogels (10 mg/mL) as storage at 37 °C. (B) Evaluation of the conversion of Y(Idm)EEH, Y(Idm)EEK and Y(Idm)EER (0.2 mg/mL) into native Idm in phosphate buffered saline (PBS, pH 7.4) at 37 °C. $^{**}P = 0.0087$, Y(Idm)EEK *vs.* Y(Idm)EE; $^{**}P = 0.0070$, Y(Idm)EER *vs.* Y(Idm)EEH.

Declaration of competing interest

We declare that we have no financial and personal relationships with other people or organizations that can inappropriately influence our work, there is no professional or other personal interest of any nature or kind in any product, service and/or company that could be construed as influencing the position presented in, or the review of, the manuscript entitled “Autocatalytic strategy for tunning drug release from peptide-drug supramolecular hydrogel”.

Acknowledgment

This work is financially supported by the Natural Science Foundation of Zhejiang Province (No. LY20H180012).

Supplementary materials

Supplementary material associated with this article can be found, in the online version, at doi:10.1016/j.cclet.2023.108209.

References

[1] Y. Wang, A.G. Cheetham, G. Angacian, et al., Adv. Drug Deliv. Rev. 110 (2017) 112–126.
[2] B.M. Cooper, J. Iegre, D.H. O'Donovan, et al., Chem. Soc. Rev. 50 (2021) 1480–1494.
[3] F. Zhao, M.L. Ma, B. Xu, Chem. Soc. Rev. 38 (2009) 883–891.
[4] X. Yang, Z. Cao, H. Lu, H. Wang, Adv. Healthc. Mater. 10 (2021) e2100381.
[5] Y. Zhang, T. Li, Y. Hu, et al., Chin. Chem. Lett. 33 (2022) 2507–2511.
[6] D.J. Worm, S. Els-Heindl, A.G. Beck-Sickinger, Pept. Sci. 112 (2020) e24171.
[7] J. Rautio, H. Kumpulainen, T. Heimbach, et al., Nat. Rev. Drug Discov. 7 (2008) 255–270.
[8] H. Wang, Z. Yang, Nanoscale 4 (2012) 5259–5267.
[9] G. Liang, Z. Yang, R. Zhang, et al., Langmuir 25 (2009) 8419–8422.
[10] H. Wang, Z. Feng, B. Xu, Adv. Drug Deliv. Rev. 110 (2017) 102–111.
[11] X.L. Li, H. Liu, A.L. Yu, et al., Chin. Chem. Lett. 32 (2021) 3936–3939.
[12] I. Vhora, S. Patil, P. Bhatt, A. Misra, Adv. Protein Chem. Struct. Biol. 98 (2015) 1–55.
[13] K. Fosgerau, T. Hoffmann, Drug Discov. Today 20 (2015) 122–128.
[14] Z. Zhang, S. Ai, Z. Yang, X. Li, Adv. Drug Deliv. Rev. 174 (2021) 482–503.
[15] Y. Fang, H. Wang, Pharmaceutics 14 (2022) 212.
[16] J. Li, Y. Fang, Y. Zhang, et al., Adv. Mater. 33 (2021) e2008518.
[17] J. Li, Z.S. Wang, H.H. Li, et al., Chin. Chem. Lett. 33 (2022) 1936–1940.
[18] S.H. Hiew, J.K. Wang, K. Koh, et al., Acta Biomater. 136 (2021) 111–123.
[19] Y.M. Zhang, Y.H. Ding, X.X. Li, et al., Chin. Chem. Lett. 32 (2021) 3636–3640.

[20] T. Liu, G.T. Liu, J.H. Zhang, et al., Chin. Chem. Lett. 33 (2022) 1880–1884.
[21] D. Böhme, A.G. Beck-Sickinger, ChemMedChem 10 (2015) 804–814.
[22] J. van Gelder, M. Shafiee, E. De Clercq, et al., Int. J. Pharm. 205 (2000) 93–100.
[23] M. Alas, A. Saghaeidehkordi, K. Kaur, J. Med. Chem. 64 (2021) 216–232.
[24] B.M. Liederer, R.T. Borchardt, J. Pharm. Sci. 95 (2006) 1177–1195.
[25] A.M. Garcia, M. Kurbasic, S. Kralj, et al., Chem. Commun. 53 (2017) 8110–8113.
[26] A. Ochoa-Solano, G. Romero, C. Gitler, Science 156 (1967) 1243–1244.
[27] N. Singh, M.P. Conte, R.V. Ulijn, et al., Chem. Commun. 51 (2015) 13213–13216.
[28] J.R. Fores, M. Criado-Gonzalez, A. Chaumont, et al., Angew. Chem. Int. Ed. 58 (2019) 18817–18822.
[29] J.R. Fores, M. Criado-Gonzalez, A. Chaumont, et al., Angew. Chem. Int. Ed. 59 (2020) 14558–14563.
[30] M.O. Guler, S.I. Stupp, J. Am. Chem. Soc. 129 (2007) 12082–12083.
[31] C.B. Yang, H.M. Wang, D.X. Li, L. Wang, Chin. J. Chem. 31 (2013) 494–500.
[32] C. Zhang, X. Xue, Q. Luo, et al., ACS Nano 8 (2014) 11715–11723.
[33] M. Bélières, N. Chouini-Lalanne, C. Déjugnat, RSC Adv. 5 (2015) 35830–35842.
[34] Y.H. Ting, H.J. Chen, W.J. Cheng, J.C. Horng, Biomacromolecules 19 (2018) 2629–2637.
[35] Z. Zhang, X. Ma, T. Xia, et al., J. Biomed. Nanotechnol. 17 (2021) 1417–1425.
[36] Y. Hu, Y. Wang, J. Deng, et al., J. Control. Release 344 (2022) 261–271.
[37] H. Liu, X. Bi, Y. Wu, et al., Acta Biomater. 131 (2021) 162–171.